A Basic AC Power Flow Based on the Bus Admittance Matrix Incorporating Loads and Generators Including Slack Bus

Roberto Benato, *Senior Member, IEEE*

***Abstract*—This paper presents an algorithm for solving the AC basic power flow based on some enrichments provided in the bus admittance matrix methods findable in the literature. In particular, the interpretation of the slack bus generator as a current source rather than a voltage one and its inclusion inside an "all-inclusive" admittance matrix allows obtaining strong performances of the algorithm. In fact, this method gives both a well conditioning of the admittance matrix and the reduction of matrix partitioning for each iteration. As a result, a greater precision of the solution, a shorter execution time compared to classical commercial methods, a decreasing number of iterations and optimal convergence properties are obtained. Eventually, in order to show the efficiency of the method, real and fictious networks are tested, by comparing its results and performances with robust open source/commercial software packages that use well-known methods (*i.e.*, Newton-Raphson and Fast Decoupled Load Flow methods).**

***Index Terms*—AC basic power flow, correcting current method, iterative methods, nodal admittance matrix.**

NOMENCLATURE

A. Sets and Indices

G	Set of generator buses $a \div g$
L	Set of load buses $h \div m$
a	Slack-bus
N	Passive network
S	Shunt branches
1, 2, …, k	First, second, …, *k-th* iteration
0	Initial estimate
$\_q$	Quadrature component
$\underline{\boldsymbol{Y}}$, $\underline{\boldsymbol{Y}}_N$, $\underline{\boldsymbol{Y}}_{N\_ideal}$, $\underline{\boldsymbol{Y}}_{SGL}$	Total bus admittance, network admittance, ideal network admittance, shunt admittance matrices
$\underline{\boldsymbol{Y}}_G$, $\underline{\boldsymbol{Y}}_L$	Generator and load admittance submatrices
$\underline{\boldsymbol{Y}}_{GG}$, $\underline{\boldsymbol{Y}}_{GL}$, $\underline{\boldsymbol{Y}}_{LG}$, $\underline{\boldsymbol{Y}}_{LL}$	Admittance submatrices of $\underline{\boldsymbol{Y}}$
$\underline{\boldsymbol{Y}}_{Geq}$, $\underline{\boldsymbol{Z}}_{Geq}$	Admittance and impedance equivalent matrices as seen at generator busses
$\mathbf{1}$	Array of ones
$\underline{\Delta \boldsymbol{i}}$	Correcting current vectors
$\delta_b \ldots \delta_g$	Set of $b \div g$ generator voltage angles
$\underline{\boldsymbol{T}}_{\boldsymbol{x}}$	Transformation matrix
$diag(\underline{\boldsymbol{X}})$	Main diagonal vector of $\underline{\boldsymbol{X}}$

B. Variables and Parameters

$\underline{u}$	Complex voltage
$\lvert\underline{u}\rvert$	Voltage magnitude
$\underline{u}_{a,r}$	Constrained slack bus voltage phasor
$\underline{i}$	Complex nodal current
$\underline{y}$	Complex admittance
$\underline{S}$	Complex power
p	Active power
q	Reactive power
n_G	Number of generator buses
r	Constrained value
c	Corrected value
n_L	Number of load buses

C. Symbols

t	Transposition
$*$	Complex conjugate
$^{-1}$	Matrix inversion
$\div$	From … to …
$\otimes$	Hadamard element-wise multiplication
$/$	Element-wise division
Im	Imaginary part of a complex quantity

D. Acronyms

PFPD	**P**ower **F**low of the University of **P**a**d**ova
N-R	**N**ewton-**R**aphson
FDLF	**F**ast **D**ecoupled **L**oad **F**low
OLTC	**O**n **L**oad **T**ap **C**hanger
PST	**P**hase **S**hift **T**ransformer
DIgPF	**DIg**SILENT **P**ower**F**actory
ITER.	Number of **iter**ations
PF[17]	**P**ower **F**low presented in **[17]**

Manuscript received February 1, 2021; revised May 25, 2021 and August 3, 2021; accepted August 9, 2021. Date of publication August 11, 2021; date of current version March 28, 2022. Paper no. TPWRS-00182-2021.

The author is with the Department of Industrial Engineering, University of Padova, 35131 Padova, Italy (e-mail: roberto.benato@unipd.it).

Color versions of one or more figures in this article are available at https://doi.org/10.1109/TPWRS.2021.3104097.

Digital Object Identifier 10.1109/TPWRS.2021.3104097

I. INTRODUCTION

AC SINGLE-PHASE power flow is one of the most fascinating and important topics of power systems analysis. The knowledge of voltage magnitudes and angles of each node of an electrical grid together with active and reactive power flow through its elements (lines, and transformers) gives an immediate picture of the power system steady-state regime. This picture

allows verifying possible under/over voltages with respect to the rated values, ampacity exceeding, and other features necessary for the suitable operation of a power system.

After the first contributions (dated 1963) about power flow solution by impedance/admittance matrix iterative methods (*e.g.*, [1], [2]), with slow convergence and high demanding computer memory (chiefly the impedance matrix based methods), some monumental contributions, in technical literature, definitively declared the supremacy of N-R-based methods (*e.g.*, [3]–[7]). Successively, the topic has been highly investigated in many directions *e.g.*, ill-conditioned systems [8], [9], optimal power flow [10]–[13], AC/DC power flow with inclusion of HVDC-LCC and then HVDC-VSC [14]–[16].

However, these researches are always based on N-R and derived.

In 2001, the author has co-authored a paper published in **E**uropean **T**ransactions on **E**lectrical **P**ower [17] where a new iterative algorithm for solving AC single-phase power flow is expounded in detail for self-implementation. This algorithm did not make use of numerical analysis techniques *e.g.*, N-R method and derived. In fact, the method was based on the idea of representing both generators (excluding the slack one) and loads by means of shunt admittances with negative or positive conductances, embedded into the bus admittance matrix.

It is also worth reminding the approaches based on the AC power flow representation in conic format [18], [19] and convex relaxation technique [20]–[23]. Both are very different from the author's approach: [18] is an analytical approach based on convex relaxation which is tightened by using appropriate perturbation functions along with a network reconfiguration scheme; [20] is still an approximation of the AC power flow equations. The present method is not a numerical approach solving a non-linear problem but a circuital one which makes large use of admittance matrixes and of correcting current vectors without any perturbation function, any reconfiguration scheme, any convex relaxation and conic format. Moreover, it is also worth mentioning the approaches based on the sparse tableau formulation (STF) [24] since they are alternatives to the bus admittance matrix. These methods are diametrically opposed to that presented in this paper.

The author is still convinced of the change of the paradigm due to [17]. This conviction is testified by the directions in which [17] has been declined in the technical literature, *i.e.*, optimal power flow in distribution power networks [25], parametric analysis on distribution networks [26], different computation techniques for power flow with alternating search directions [27], power flow in unbalanced multiple-grounded 4-wire distribution networks [28], power flow for general mixed distribution networks [29], a current based model of an integrated power flow controller to be included in Newton-Raphson power flow [30] and the use of genetic algorithm to improve the high-voltage transmission system adequacy under contingency [31].

Anyway, the author was dissatisfied with some issues pertaining [17]. The first and more important issue is: why all the generators are included (with their negative conductance) in the shunt admittance matrix except the slack generator? Is it possible to also include the slack generator in the shunt admittance matrix? Is it possible to apply the correcting current vector also to the slack bus? In [17], the lack of slack generator insertion inside the shunt admittance matrix brings to an unnecessary partition of the equivalent matrix as seen at generator buses. In [17], four matrixes are introduced i.e $\underline{\mathbf{A}}$, $\underline{\mathbf{B}}$, $\underline{\mathbf{C}}$, $\underline{\mathbf{D}}$ which is a misleading choice since they make confusion with the *ABCD* hybrid matrix or transmission matrix. The formulae are cumbersome, and less evident than the present ones. Moreover, another great drawback of [17] is its application/validation only to/by fictitious grids and not to/by real ones, without considering all the elements belonging to a real grid *i.e.*, OLTCs, PSTs, distributed generation, transnational interties, voltage regulation shunt elements (capacitor banks or shunt/series reactors) and the capability curves of the generators.

This limitation is overcome and resolved by the present paper by applying the algorithm to real world grids (Sicily, South Italy, and Italy), which hold the devices described in Appendix A.

The old methods [1], [2] involving the direct use of admittance matrix have been long-abandoned due to the ill-conditioning of it since the branch admittances could be greater than the shunt ones. In fact, a network with shunt admittances, which are small with respect to the other branch admittances, is likely to be ill-conditioned, and the conditioning tends to improve with the size of the shunt admittances, *i.e.*, with the electrical connection between the network busbars and the reference node.

With the present algorithm (in the following it is named PFPD) the inclusion in the admittance matrix of the shunt admittances of all the generators (including slack one) and loads renders it well-conditioned since these shunt admittances are larger than the branch admittances depending upon the generated and absorbed complex power. This process is further improved by adding a shunt admittance due to the slack generator. This novel idea is based on the formal possibility of considering the slack generator as a quasi-ideal current source with a large but not infinite shunt admittance. It is not a theoretical enforcing but an intuition which revitalizes the direct use of admittance matrix in power flow: the bus admittance matrix is always well conditioned even with low-load and low-generation due to the presence of a strong link to ground due to the slack bus. Moreover, considering the slack generator as a current source allows the use of a correcting current vector also for it, this thing being impossible with the slack generator as a voltage source. By using either a voltage source or a current source, the constrained voltage phasor is always applied at the slack bus terminals. After twenty years, the algorithm firstly presented in [17], reaches its final form *i.e.*, PFPD.

Eventually, the slack bus is included in the shunt admittance matrix by using a source transformation, *i.e.*, by passing from a voltage source (Thevenin's equivalent generator) to a current source (Norton's equivalent generator): the algorithm reaches convergence with five iterated formulae. This intuition renders the system well-conditioned and decreases the number of the iterations and consequently the CPU times. From an electric engineering standpoint, this kind of power flow solution is more in tune with the electric nature of the problem without resorting to numerical analysis techniques.

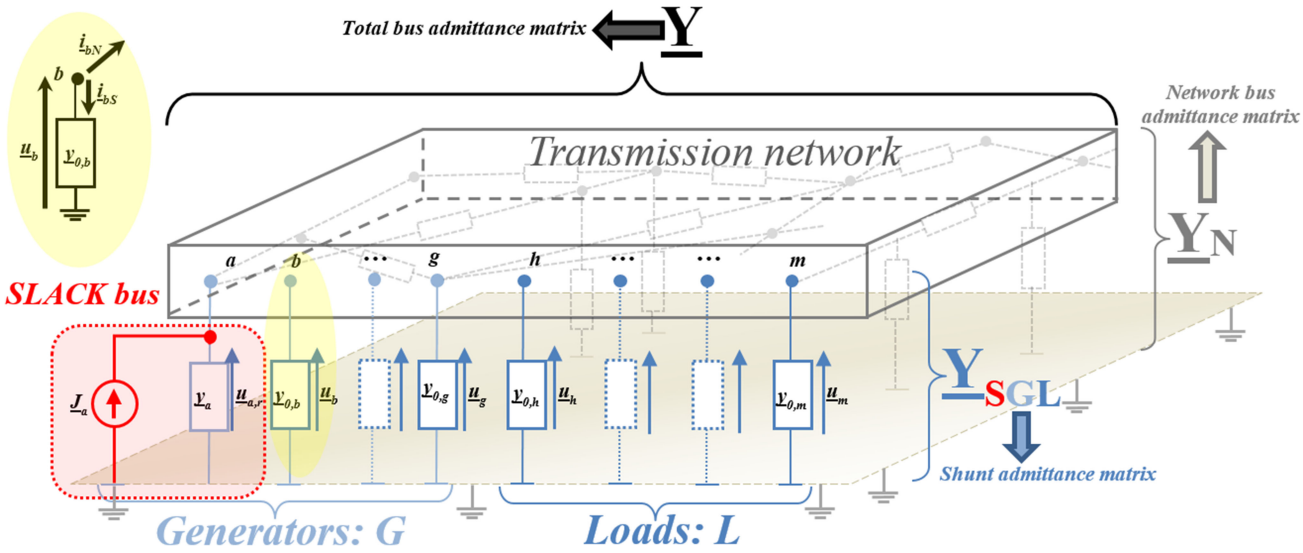

Fig. 1. Schematic representation of the power system (G: PV nodes (a: slack-generator), L: PQ nodes).

To have a wide and necessary comparison with other methods, the paper considers two reference software: the commercial DigSilent Power Factory [32] and the open-access MatPower [33] which runs in Matlab environment. Both are based on the N-R method, but the former is an optimized commercial software and the latter is composed of self-made open source and open access Matlab procedures. In this sense, MatPower looks like PFPD. The use of Matlab both to implement power flow and to study power system dynamics is well witnessed by many papers, *e.g.*, [33]–[38].

II. Novel Power Flow Algorithm With Slack Generator Inclusion in the $\underline{Y}_{\mathrm{SGL}}$ Admittance Matrix

Under the hypothesis of a symmetric and balanced three-phase power system, the equivalent single-circuit at the positive sequence can be licitly considered.

The classical formulation of AC single-phase power flow consists in defining the following constraints:

1) **PV buses**, where injected active power $p_{b,r} \ldots p_{g,r}$ and voltage magnitudes $|\underline{u}_{b,r}| \ldots |\underline{u}_{g,r}|$ are constrained;
2) **PQ buses**, where absorbed complex power (even null) $p_{h,r}+jq_{h,r} \ldots p_{m,r}+jq_{m,r}$ are constrained;
3) A **SLACK bus**, which has a constrained reference voltage phasor, *i.e.*, $\underline{u}_{a,r}=u_{a,r}e^{j0}$.

The method is based on the idea of representing both all generators (including the slack one) and loads by means of shunt admittances with negative or positive conductances and to embed them into the bus admittance matrix.

By considering, firstly, a generic load bus *m*, if $\underline{S}_m=p_{\mathrm{m}}+jq_{\mathrm{m}}$ is the complex power (even null) absorbed, it results

$$\underline{S}_m=\underline{u}_m\underline{i}_{mS}^*;\quad \underline{i}_{mS}=\frac{\underline{S}_m^*}{\underline{u}_m^*}=\underline{y}_m\underline{u}_m;\quad \underline{y}_m=\frac{p_m-jq_m}{|\underline{u}_m|^2} \tag{1}$$

when the voltage $\underline{u}_m$ is applied.

Similarly, by taking into consideration a generic generator bus *g*, if $\underline{S}_g=p_g+jq_g$, is the complex power injected, it is possible to theoretically represent it by a complex admittance $\underline{y}_g$, *i.e.*,

$$\underline{S}_g=-\underline{u}_g\underline{i}_{gS}^*;\quad \underline{i}_{gS}=-\frac{\underline{S}_g^*}{\underline{u}_g^*}=\underline{y}_g\underline{u}_g;\quad \underline{y}_g=\frac{-p_g+jq_g}{|\underline{u}_g|^2} \tag{2}$$

with a nodal voltage equal to $\underline{u}_g$. The elements belonging to the electrical network, *e.g.*, lines, transformers, shunt reactors, shunt capacitors are included in the network bus admittance $(n_G+n_L)\times(n_G+n_L)$ matrix $\underline{\boldsymbol{Y}}_{\boldsymbol{N}}$ so that (3) yields (by referring to the symbols shown in Fig. 1)

$$\underline{\boldsymbol{i}}_{\boldsymbol{N}}=\underline{\boldsymbol{Y}}_{\boldsymbol{N}}\underline{\boldsymbol{u}} \tag{3}$$

where:

$$\underline{\boldsymbol{i}}_{\mathbf{N}}=\left[\underline{i}_{aN}\,|\,\underline{i}_{bN}\,|\,\ldots.\,|\,\underline{i}_{gN}\,|\,\underline{i}_{hN}\,|\,\ldots.\,|\,\ldots.\,|\,\ldots.\,|\,\underline{i}_{mN}\right]^t \tag{4}$$

$$\underline{\boldsymbol{u}}=\left[\underline{u}_{a,r}\,|\,\underline{u}_b\,|\,\ldots.\,|\,\underline{u}_g\,|\,\underline{u}_h\,|\,\ldots.\,|\,\ldots.\,|\,\ldots.\,|\,\underline{u}_m\right]^t \tag{5}$$

The elements representing the constraints, *i.e.*, slack bus, PV (generators), PQ (loads) are included in another $(n_G+n_L)\times(n_G+n_L)$ square diagonal shunt admittance matrix named $\underline{\mathbf{Y}}_{\boldsymbol{SGL}}$.

This matrix holds the shunt (S in the following) branches and can be partitioned as shown in Fig. 2.

As it is detailed in the following, the value of $\underline{y}_a$ can be fixed to a large value *e.g.*, -j·10^5 p.u.

For the S block it is possible to write (6):

$$\underline{\boldsymbol{i}}_{\boldsymbol{S}}=\underline{\boldsymbol{Y}}_{\boldsymbol{SGL}}\underline{\boldsymbol{u}} \tag{6}$$

where $\underline{\boldsymbol{i}}_{\mathbf{S}}=\left[\underline{i}_{aS}\,|\,\underline{i}_{bS}\,|\,\ldots.\,|\,\underline{i}_{gS}\,|\,\underline{i}_{hS}\,|\,\ldots.\,|\,\ldots.\,|\,\ldots.\,|\,\underline{i}_{mS}\right]^t$.

By summing member-to-member (3) and (6), it is possible to write (7) *i.e.*,:

$$\underline{\boldsymbol{i}}=\underline{\boldsymbol{Y}}\,\underline{\boldsymbol{u}} \tag{7}$$

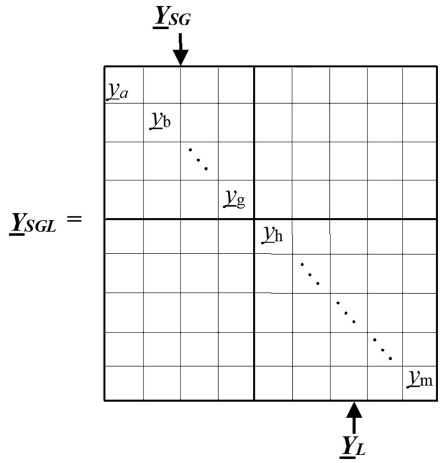

Fig. 2. Partitioned slack-generator-load square diagonal shunt admittance matrix.

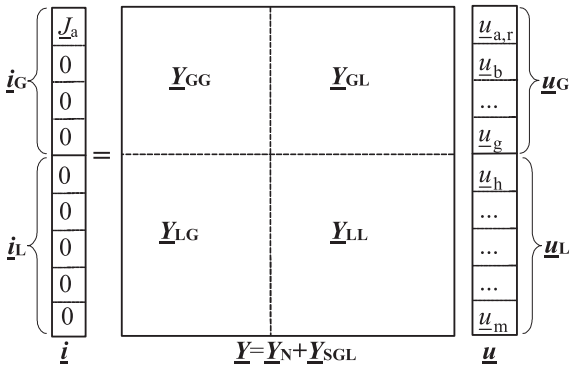

Fig. 3. Partitioned form of $\underline{i}=\underline{Y}\,\underline{u}$.

where $\underline{Y}=\underline{Y}_N+\underline{Y}_{SGL}$ is the total bus admittance matrix. It is worth noting that $\underline{i}=\left[\underline{J}_a\,|\,0\,|\,0\,|\,0\,|\,0\,|\,0\,|\,0\,|\,0\,|\,0\right]^t$ is the column vector of the currents injected at $a \div m$ buses in Fig. 1.

By introducing the partition shown in Fig. 3, it follows:

$$\underline{i}_G = \underline{Y}_{GG}\underline{u}_G + \underline{Y}_{GL}\underline{u}_L \tag{8}$$

$$\mathbf{0} = \underline{Y}_{LG}\underline{u}_G + \underline{Y}_{LL}\underline{u}_L. \tag{9}$$

By applying the standard matrix procedure for variable elimination, (9) can be rewritten as

$$\underline{u}_L = -\,\underline{Y}_{LL}^{-1}\,\underline{Y}_{LG}\,\underline{u}_G \tag{10}$$

The substitution of $\underline{u}_L$ in (8) yields:

$$\underline{i}_G = \left[\underline{Y}_{GG} - \underline{Y}_{GL}\underline{Y}_{LL}^{-1}\underline{Y}_{LG}\right]\underline{u}_G = \underline{Y}_{Geq}\underline{u}_G \tag{11}$$

where $\underline{Y}_{Geq}$ allows, by means of its inverse, computing the impedance matrix as seen at the generator buses *i.e.*,

$$\underline{Z}_{Geq} = \underline{Y}_{Geq}^{-1}. \tag{12}$$

The element $\underline{Z}_{\mathrm{Geq}}(1,1)$ of this matrix is the impedance as seen at slack bus and can give the current source $\underline{J}_a$ by means of:

$$\underline{J}_a = \underline{u}_{a,r} \big/ \underline{Z}_{Geq}\,(1,1) \tag{13}$$

It should be noted that the matrix partitioning of $\underline{Y}_{Geq}$ and the consequent cumbersome plethora of formulae is avoided differently from [17] (for the comparison see Appendix B and for the computational effects/improvements see Section III.A). This possibility derives from a source transformation as shown in Fig. 4.

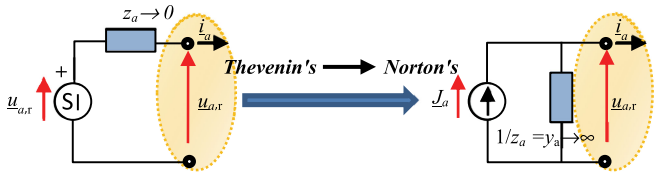

Fig. 4. Source transformation for slack-bus: from Thevenin's voltage source (as used in [17]) to Norton's current source.

Paper [17] considered the slack bus as an ideal voltage source with a zero impedance in series (the Thevenin's generator) which gave the slack-bus a different treatment from the other generators of the grid. On the contrary, if the slack-bus is considered as a current source (the Norton's generator), its internal admittance $\underline{y}_a$ can be considered inside the $\underline{Y}_{SGL}$ exactly like the other shunt branches.

This strongly simplifies the algorithm and renders the total bus admittance matrix $\underline{Y}$ well-conditioned so to reduce the number of cycles (and CPU times) of the iterative procedure, as it is demonstrated in the following.

It is well known that the fixed busbar voltage, assumed for the slack bus, can be interpreted as an infinitely strong ground tie. J. Arrillaga writes about the slack bus [6]: "*If it is represented as a voltage source with a series impedance of zero value, and then converted to the Norton equivalent, the fictitious shunt admittance is infinite, as is the injected current.*" These words have been a source of strong inspiration for the author.

Certainly, an ideal voltage source cannot be converted into a current source, but a quasi-ideal voltage source can. By considering the Thevenin's equivalent generator of Fig. 4, the following relation can be written:

$$\lim_{|\underline{z}|\to 0+} (\underline{u}_{a,r} - \underline{z}\underline{i}_a) = \underline{u}_{a,r}$$

and the admittance in parallel with the current source of the Norton's equivalent generator given by (13) must be infinite, as in the following:

$$\left|\underline{y}_a\right| = \lim_{|\underline{z}|\to 0+} \frac{1}{|\underline{z}|} = +\infty$$

In calculus, the "infinity" of the above limit refers to an arbitrarily large value. In fact, $\underline{y}_a$ can be made arbitrarily large by requiring $|\underline{z}|$ to be close enough to zero [39].

Therefore, from a numerical point of view, the slack admittance must assume a large value in comparison with the other generator/load admittances.

For this purpose, many tests on different networks demonstrate that two orders of magnitude greater than the other network admittances are sufficient to make the algorithm converge to the exact solution.

In fact, it is fundamental that, at the terminals of the slack bus, the constrained voltage phasor must be always applied (see the detail inside the dashed/shadowed ellipses of Fig. 4): this is

verified by means of both a voltage source and a current one. For PFPD, it is more convenient the use of the current source since the shunt admittance $\underline{y}_a$ can be embedded inside the $\underline{\boldsymbol{Y}}_{SGL}$.

A. Iterative Procedure and Convergence Criterion

The iterative procedure does not need any numerical analysis technique. The initial values of the admittances in the matrix $\underline{\boldsymbol{Y}}_{SGL}$ can be set equal to:

For SLACK-bus: $\underline{y}_a = -j\cdot 10^5$ p.u.

The slack admittance $\underline{y}_a$, as already mentioned, must be an arbitrarily large value. The value of -j10^5 is conventionally chosen in order not to badly scale the $\underline{\boldsymbol{Y}}_{SGL}$ matrix. However, several tests have been made to verify the convergence performances of the algorithm (ITER. and CPU times). They show the same convergence behaviour even for different values of $\underline{y}_a$ (from -j10^2 to -j10^{16} p.u.). Thus, the algorithm is not sensitive to the choice of the slack admittance value, by assuming values of $|\,\underline{y}_a\,|$ greater than 10^2. However, this fact agrees with the above-mentioned theory: the admittance must be sufficiently large in comparison with the other generator and load admittances (whose order of magnitude is typically about 10^0 p.u.). It is worth noting that $\underline{y}_a$ is a negative imaginary number: this is due to the assumption of a pure inductive shunt admittance for the slack generator. From a mathematical standpoint, the well conditioning of $\underline{\boldsymbol{Y}}$ is attributable to the presence of a strong tie to ground due to the slack admittance: this ensures the matrix invertibility.

For PQ buses: with nominal $|\underline{u}_{h0}|\ldots|\underline{u}_{m0}|=1$ p.u., the load admittances are computed as in (14):

$$\underline{y}_{h0}=\frac{p_{h,r}}{|\underline{u}_{h0}|^2}-j\frac{q_{h,r}}{|\underline{u}_{h0}|^2};\ldots;\underline{y}_{m0}=\frac{p_{m,r}}{|\underline{u}_{m0}|^2}-j\frac{q_{m,r}}{|\underline{u}_{m0}|^2}. \quad (14)$$

In this way, the PQ admittances are modelled by assuming that they absorb the constrained power $p_{h,r}\div p_{m,r}$ and $q_{h,r}\div q_{m,r}$ at their nominal voltage (1 p.u.). These values of admittances are necessary to build the iterative load correcting current vector; consequently, these values are not updated during the iterative procedure.

For PV buses:

$$\underline{y}_{b0}=-\frac{p_{b,r}}{\left|\underline{u}_{b,r}\right|^2}+j\frac{q_{b0}}{\left|\underline{u}_{b,r}\right|^2};\ldots;\underline{y}_{g0}=-\frac{p_{g,r}}{\left|\underline{u}_{g,r}\right|^2}+j\frac{q_{g0}}{\left|\underline{u}_{g,r}\right|^2}. \quad (15)$$

Also, for PFPD as for any iterative method, a good initial guess is needed to start the iterative process [40] and it is fundamental for the convergence to the exact solution. It is worth remembering that in (15) $p_{b,r}\div p_{g,r}$ and $|\underline{u}_{b,r}|\div|\underline{u}_{g,r}|$ are the constrained quantities of the PV nodes. The only unconstrained quantities in (15), are $q_{b0}\div q_{g0}$ which need an initial guess.

They are estimated by considering the network as ideal (i.e $\underline{\boldsymbol{Y}}_{N\_ideal}$ with only imaginary elements) and by including in the matrix $\underline{\boldsymbol{Y}}_{SGL}$ only the PQ buses (see Fig. 5) with their nominal admittances (*i.e.*, $|\underline{u}_{h0}|\ldots|\underline{u}_{m0}|=1$ p.u.). All the generator voltage phasors have magnitude equal to the constrained values and zero angles. Equation (11) immediately gives $\underline{\boldsymbol{i}}_G$, and the consequent reactive power initial guess $q_{b0}\div q_{g0}$. As a matter of fact, these estimates are based on a flat start (see Fig. 5).

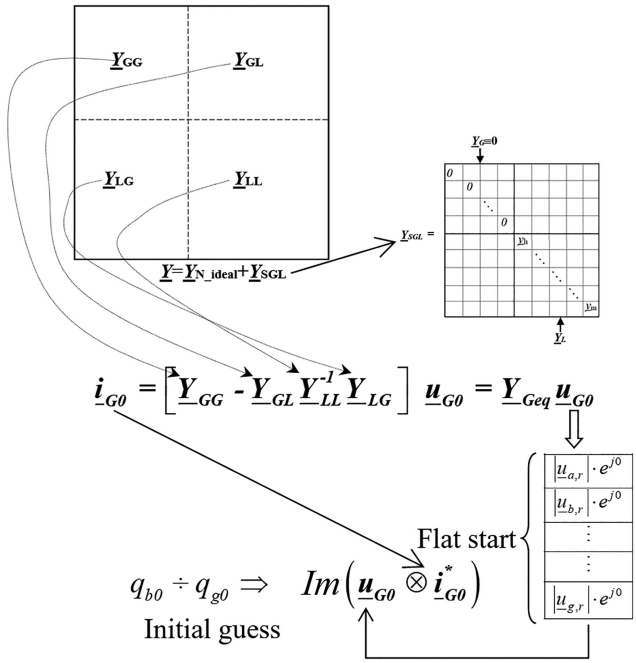

Fig. 5. Initial guess of the generator reactive power $q_{b0}\div q_{g0}$.

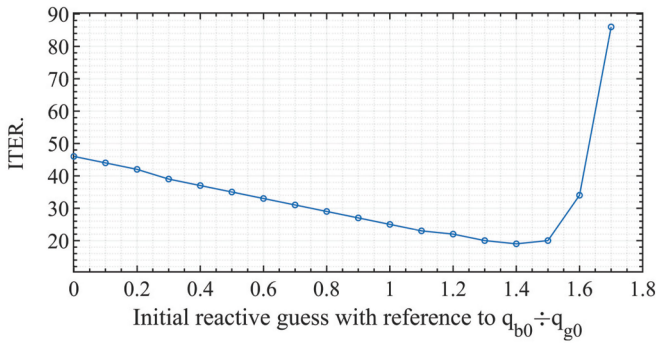

Fig. 6. Region of attraction for the 1325-bus Italian grid (10^{-8} p.u. convergence tolerance).

In theory, the only way to know if a given initial guess is adequate for obtaining a solution of a power flow method is to determine the region of attraction of the solution [40]. In case of PFPD, the regions of attraction like the ones shown in [40], [41] cannot be determined, since in PFPD the only initial values are the reactive power $q_{b0}\div q_{g0}$ of the PV generators. Therefore, Fig. 6 shows the region of attraction by varying the initial reactive values of the generators with reference to the initial guess $q_{b0}\div q_{g0}$ as explained above (in Fig. 6 $q_{b0}\div q_{g0}$ is indicated as 1). The specific tested network is the Italian grid but all the regions of attraction of the other networks show a similar behaviour. However, the minimum number of iterations fall in a range 0.6-1.4 $q_{b0}\div q_{g0}$ testifying that the choice of $q_{b0}\div q_{g0}$ is effective to obtain a low ITER.

The iterative procedure is based on the suitable injections into the grid buses of correcting current vectors $\underline{\Delta\boldsymbol{i}}_G$ and $\underline{\Delta\boldsymbol{i}}_L$. In order to reach the convergence, the following formulae (16)÷(20) are applied sequentially, as depicted in the flow-chart of Fig. 7. These formulae are referred to the first iteration, but 1 and 0

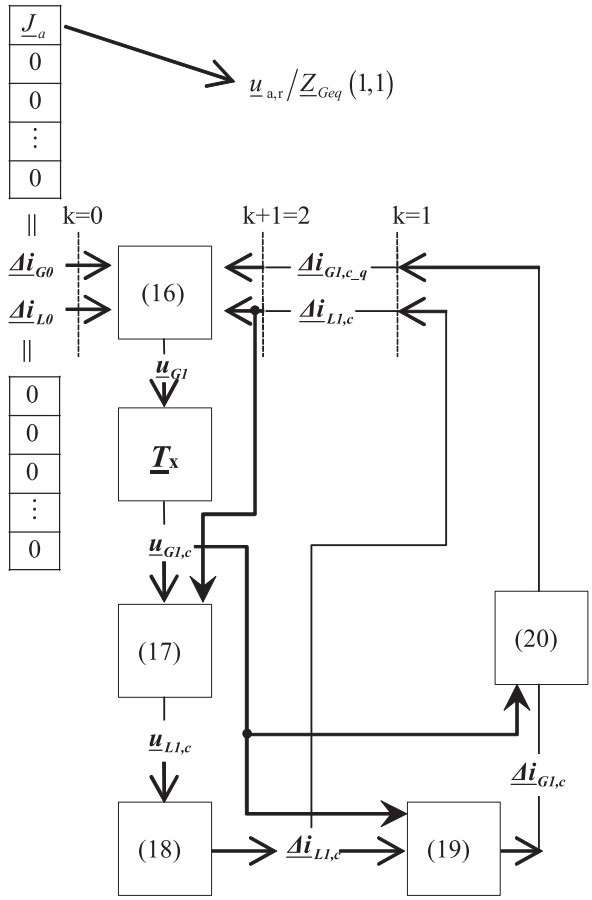

Fig. 7. Flow chart of the novel algorithm for k = 1.

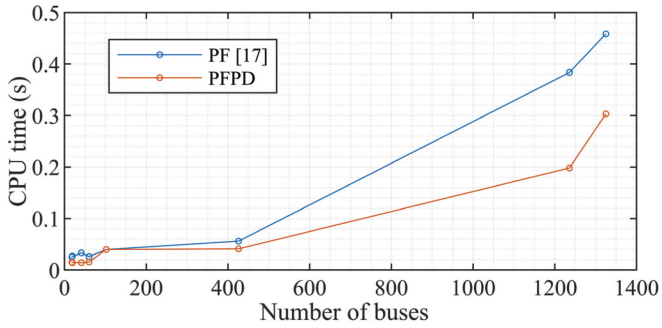

Fig. 8. CPU time comparisons between PFPD and PF[17], with 10^{-8} p.u. maximum active/reactive power mismatches.

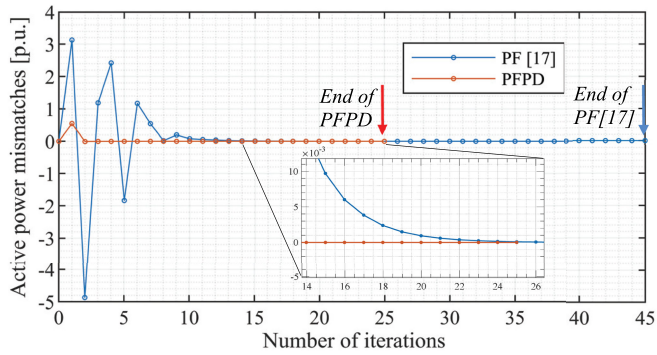

Fig. 9. Comparison between PFPD and PF[17] of the maximum nodal active mismatches of the 1325-bus Italian grid for a 10^{-8} p.u. convergence tolerance.

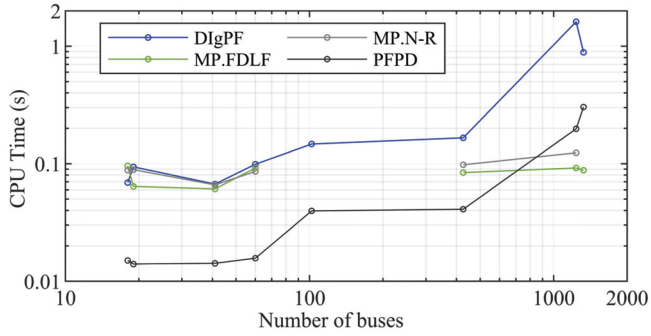

Fig. 10. CPU time comparisons among PFPD, DIgPF, MP.FDLF and MP.N-R with 10^{-8} p.u. maximum active/reactive power mismatches.

subscripts are omitted for the sake of clarity.

$$\underline{u}_G = \underline{Z}_{Geq}\left(\Delta\underline{i}_{G,c\_q} - \underline{Y}_{GL}\underline{Y}_{LL}^{-1}\Delta\underline{i}_{L,c}\right) \quad (16)$$

$$\underline{u}_{L,c} = -\underline{Y}_{LL}^{-1}\underline{Y}_{LG}\underline{u}_{G,c} + \underline{Y}_{LL}^{-1}\Delta\underline{i}_{L,c} \quad (17)$$

$$\Delta\underline{i}_{L,c} = -diag\left(\underline{Y}_L\right) \otimes \left(\mathbf{1} - \left|\underline{u}_{L,c}\right|^2\right) \Big/ \underline{u}_{L,c}^* \quad (18)$$

$$\Delta\underline{i}_{G,c} = \underline{Y}_{Geq}\underline{u}_{G,c} + \underline{Y}_{GL}\underline{Y}_{LL}^{-1}\Delta\underline{i}_{L,c} \quad (19)$$

$$\Delta\underline{i}_{G,c\_q} = -j\left[Im\left(\underline{u}_{G,c} \otimes \Delta\underline{i}_{G,c}^*\right)\right] \Big/ \underline{u}_{G,c}^* \quad (20)$$

For the slack bus, (20) must not be applied (since both active and reactive power of the slack generator are unknow quantities) so that:

$$\Delta\underline{i}_{G,c\_q}(1,1) = \Delta\underline{i}_{G,c}(1,1)$$

Equations (16), (17) and (19) are the generalization of (8) and (9), once the correcting current vectors $\Delta\underline{i}_{G,c}$ and $\Delta\underline{i}_{L,c}$ are considered. For (18) and (20) see Appendix B.

In order to start with the first cycle ($k = 1$), it is necessary to give $\Delta\underline{i}_{G0}$ all zero values but the first one which is equal to the slack bus current source $\underline{J}_a$, and $\Delta\underline{i}_{L0}$ all zero values (see Fig. 6). Equation (16) yields the voltage vector $\underline{u}_{G1}$: it has got magnitudes different from the constrained ones. Therefore, by $\underline{T}_x$ matrix shown in Fig. 7, a new corrected vector $\underline{u}_{G1,c}$ can be built by changing the calculated voltage magnitudes with the constrained ones but by leaving $\delta_b \ldots \delta_g$ angles unchanged.

The corrected load vector $\underline{u}_{L1,c}$ is obtainable from (17) and can determine, by (18), the correcting load current vector $\Delta\underline{i}_{L1,c}$, which enters into (19) so giving the correcting generator current vector $\Delta\underline{i}_{G1,c\_q}$. Since the generator corrections must involve the reactive power, the quadrature component $\Delta\underline{i}_{G1,c\_q}$ is derived by means of (20). This procedure is iterated until convergence, *i.e.*, until any mismatch of load active and reactive power is within the tolerance. It is impressive and fascinating how five iterated formulae without resorting to Jacobian matrix and any real/imaginary decomposition (as in FDLF) solve the power flow of any power system.

TABLE I
CPU TIMES AND ITER. FOR NEW PFPD AND OLD PF[17] WITH MAXIMUM ACTIVE/REACTIVE POWER MISMATCHES UP TO 10^{-8} P.U. (1 W/VAR) PC: INTEL(R) XEON(R) GOLD 5222 CPU @ 3.80 GHZ, RAM: 384 GB

	PF[17] Year: 2001		PFPD Year: 2021	
Network	***ITER.***	***CPU (s)***	***ITER.***	***CPU (s)***
18-bus	13	0.025	13	0.015
19-bus	18	0.027	13	0.014
41-bus	15	0.033	14	0.014
60-bus	33	0.026	20	0.016
Sicily, 102-bus (Low Load)	11	0.040	11	0.016
South-Italy, 426-bus (Low Load)	28	0.056	16	0.041
Italy, 1236-bus (Low load)	43	0.384	17	0.198
Italy, 1325-bus (High load)	45	0.459	25	0.303

TABLE II
CPU TIMES AND ITER. FOR NEW PFPD AND OLD PF[17] WITH MAXIMUM ACTIVE/REACTIVE POWER MISMATCHES UP TO 10^{-10} P.U. (0.01 W/VAR) PC: INTEL(R) XEON(R) GOLD 5222 CPU @ 3.80 GHZ, RAM: 384 GB

	PF[17] Year: 2001		PFPD Year: 2021	
Network	***ITER.***	***CPU (s)***	***ITER.***	***CPU(s)***
18-bus	17	0.025	16	0.018
19-bus	23	0.027	17	0.015
41-bus	18	0.025	8	0.014
60-bus	40	0.031	25	0.015
Sicily, 102-bus (Low Load)	14	0.024	14	0.030
South-Italy, 426-bus (Low Load)	36	0.057	19	0.067
Italy, 1236-bus (Low load)	55	0.482	21	0.247
Italy, 1325-bus (High load)	55	0.560	32	0.415

III. COMPARISONS BETWEEN PFPD AND OTHER METHODS

A. Preliminary Comparison Between the New PFPD and the Old PF[17]

PFPD is implemented in Matlab environment and tested for several transmission grids, which differ in topologies and load/generation scenarios. In particular, real networks are studied: the Sicilian grid, the South-Italy grid and the entire Italian grid, with two load scenarios (low and high ones). Before the comparison between PFPD and other widely available methods, it is meaningful to provide a comparison between PFPD and PF[17] in order to show the strong enrichments and improvements brought by the change in the voltage/current source.

Tables I and II show ITER. and the CPU times of the new PFPD and the old PF[17] for two different tolerances, *i.e.*, 10^{-8} p.u. and 10^{-10} p.u. They are excessively low tolerances, but they show the great accuracy of the new method. Regarding the CPU times, it is worth underlying that it always means the iterative cycle computation time and not the data preparation time. It is well known that the latter is always a small fraction of the former (in any case for the two methods the data preparation times are totally equal). The comparison clearly demonstrates that PFPD is more efficient than PF[17] with a number of iterations always fewer than PF[17] and sometimes much fewer.

In fact, as the network nodes increase, the PFPD iterations are halved with respect to PF[17]. The reduction of matrix partitioning due to the slack bus inclusion into the bus admittance matrix avoids the sparsity destruction and decreases the number of iterations. The gained computational advantage brings to a significant CPU time improvement as shown in Fig. 8. Furthermore, Fig. 9 highlights the comparison between the active power mismatches of PFPD and PF[17]. It is worth noting the more stable behaviour of the PFPD mismatches compared to those of PF[17] due to the fundamental possibility of injecting a correcting current also into the slack bus.

To assure that the novel interpretation of the slack bus generator does not cause any computational issue, different tests are presented by "stressing" the features of the above-mentioned networks.

This stressing is obtained by increasing the *r/x* ratio of all the lines, and by increasing the power absorbed by all the PQ nodes (heavy load conditions). These characteristics, in fact, could make the analysed networks ill-conditioned [42], so it is of interest to observe whether the PFPD is sensitive to them or not. Table III shows the limit to which both PF[17] and PFPD can converge with two different stress parameters.

The former is the *r/x* maximum multiplier (*i.e.*, *r/x* m.m.) applied to the resistance of each line that makes the two methods converge. It is worth noting that PFPD converges for equal or even larger values of the *r/x* ratios. The latter is the PQ maximum percentage increase (*i.e.*, PQ m.p.i.) applied to the active and reactive power that makes the two methods converge. In all the

TABLE III
R/X M.M. AND PQ M.P.I. FOR NEW PFPD AND OLD PF[17] WITH MAXIMUM ACTIVE/REACTIVE POWER MISMATCHES UP TO 10^{-8} P.U. (1 W/VAR) PC: INTEL(R) XEON(R) GOLD 5222 CPU @ 3.80 GHZ, RAM: 384 GB

	PF[17] Year: 2001		PFPD Year: 2021	
Network	***r/x m.m.***	**PQ m.p.i.**	***r/x m.m***	**PQ m.p.i.**
18-bus	7	+30%	9	+40%
19-bus	3	+290%	3	+290%
41-bus	10	+30%	11	+30%
60-bus	5	+7%	9	+20%
Sicily, 102-bus (Low Load)	10	+290%	10	+290%
South-Italy, 426-bus (Low Load)	9	+40%	9	+70%
Italy, 1236-bus (Low load)	6	+40%	6	+40%
Italy, 1325-bus (High load)	3	+2%	5	+11%

TABLE IV
CPU TIMES AND ITER. FOR DIFFERENT POWER FLOW SOLUTIONS WITH MAXIMUM ACTIVE/REACTIVE POWER MISMATCHES UP TO 10^{-8} P.U. (1 W/VAR) PC: INTEL(R) XEON(R) GOLD 5222 CPU @ 3.80 GHZ, RAM: 384 GB

	DiGS		MATPOWER				PFPD	
			FDFL		N-R			
Network	***ITER.***	***CPU (s)***	***ITER.***	***CPU (s)***	***ITER.***	***CPU (s)***	***ITER.***	***CPU (s)***
18-bus	4	0.069	8	0.096	4	0.088	13	0.015
19-bus	5	0.094	10	0.064	7	0.089	13	0.014
41-bus	4	0.067	9	0.061	4	0.066	14	0.014
60-bus	5	0.099	11	0.092	4	0.086	20	0.016
Sicily, 102-bus (Low Load)	4	0.147	NC		NC		11	0.016
South-Italy, 426-bus (Low Load)	4	0.166	28	0.084	7	0.098	16	0.041
Italy, 1236-bus (Low load)	6	1.613	14	0.092	7	0.124	17	0.198
Italy, 1325-bus (High load)	5	0.887	20	0.088	NC		25	0.303

TABLE V
CPU TIMES AND ITER. FOR DIFFERENT POWER FLOW SOLUTIONS WITH MAXIMUM ACTIVE/REACTIVE POWER MISMATCHES UP TO 10^{-10} P.U. (0.01 W/VAR) PC: INTEL(R) XEON(R) GOLD 5222 CPU @ 3.80 GHZ, RAM: 384 GB

	DiGS		MATPOWER				PFPD	
			FDFL		N-R			
Network	***ITER.***	***CPU (s)***	***ITER.***	***CPU (s)***	***ITER.***	***CPU (s)***	***ITER.***	***CPU(s)***
18-bus	4	0.065	4	0.084	10	0.085	16	0.018
19-bus	5	0.076	12	0.100	14	0.086	17	0.015
41-bus	5	0.080	9	0.065	4	0.064	8	0.014
60-bus	5	0.065	5	0.099	13	0.063	25	0.015
Sicily, 102-bus (Low Load)	4	0.198	NC		NC		14	0.030
South-Italy, 426-bus (Low Load)	4	0.176	7	0.100	NC		19	0.067
Italy, 1236-bus (Low load)	6	1.788	7	0.133	16	0.086	21	0.247
Italy, 1325-bus (High load)	5	0.877	NC		24	0.092	32	0.415

above-mentioned cases, negative computational issues are never found in PFPD.

On the contrary, better convergence properties, lower CPU times and more stable behaviour than PF [17] are observed.

B. Comparison Between PFPD and MatPower, DIgPF

In order to validate the algorithm, the power flow solutions are compared with those of well-proven software packages, in terms of performance and solution.

The comparisons are performed with two different reliable tools widely used for power flow calculations: DIgPF - a commercial software exploiting the N-R algorithm - and MATPOWER - a collection of open-source Matlab codes exploiting several solver-algorithms, including N-R and FDLF. Once defined the test grids, in order to pass data from an environment to another, some interface procedures have been developed as in [43]. Tables IV and V report the CPU times and the number of iterations of PFPD compared with DIgPF, MATPOWER, referring to two different power mismatches: 10^{-8} p.u. and 10^{-10} p.u.

TABLE VI
ORDER OF MAGNITUDE OF MINIMUM AND MAXIMUM SOLUTION DEVIATIONS AMONG PFPD, DIGPF AND MP

		Magnitude deviations [p.u.]	Angle deviations [deg]
PFPD-DIgPF	Min dev.	10^{-10}	10^{-4}
	Max dev.	10^{-3}	10^{-2}
PFPD-MP	Min dev.	10^{-5}	10^{-4}
	Max dev.	10^{-3}	10^{0}

It should be noted that CPU times for PFPD are always lower (or sometimes comparable) with those of the other considered methods. This feature is graphically confirmed by Fig. 10.

Differently from the other methods, PFPD always converges in any grid even with maximum active/reactive power mismatches equal to 10^{-8} p.u. In order to check the consistency of the solutions obtained with the different methods, a voltage phasor comparison between PFPD and DIgPF demonstrates an excellent agreement (see Table VI).

Differently, the same analysis between PFPD and MATPOWER shows slightly larger deviations between the solutions. It is

ascertained that this behaviour is due to the different models used for the transmission lines: PFPD models them as equivalent π-models with distributed parameters [44], whereas MATPOWER models them as nominal π-models with lumped parameters [33].

When dealing with grids including long transmission lines, the differences can be not negligible.

IV. Conclusion

A novel power flow solution named PFPD based on the circuit theory and not on numerical techniques (Newton-Raphson and derived) is throughout presented. All the PQ, PV nodes and the slack bus are englobed into the bus admittance matrix in the form of shunt admittances: this is possible also for slack generator since it is considered as a quasi-ideal current source. Convergence is guaranteed by the suitable injections of two correcting current vectors into all the generators including slack one and into all loads. The possibility of injecting a correcting current phasor also into the slack bus is a key feature of this method allowing robust, stable, precise, and extremely fast convergence. The conditioning of bus admittance matrix is further increased by adding a strong tie to ground due to the large shunt admittance representing the slack bus. The initial guess of the generator reactive power is explained and its influence on the convergence to an exact solution is shown *i.e.*, PFPD region of attraction. The paper highlights that the precision of PFPD (*i.e.*, active/reactive power mismatches in PQ nodes) is greater (up to 10^{-12} p.u.) and the CPU times are shorter (or comparable) than those of N-R methods either open access (Matpower) or commercial software (DiGSILENT PF). Even if PFPD has got a greater number of iterations, the time per iteration is much shorter, hence the overall CPU times of PFPD are shorter. The unnecessary decomposition of real/imaginary parts in PFPD with respect to FDLF brings to better convergence features even in ill-conditioned networks.

Further researches are ongoing to transform this basic AC power flow in a complete AC/DC power flow, including HVDC/LCC and HVDC/VSC together with optimal power flow and matrix automatic adjustment of power flow solution.

Appendix A
Inclusion of Real Network Components

In the previous paper [17], the algorithm was only applied to fictitious networks, so only two-winding transformers, lines, loads, and generators were considered. In this paper, in order to render the algorithm a useful tool, the typical devices existing in real power systems are considered.

In particular, it is necessary to model the modern scenarios (*e.g.*, distributed generation and power electronics penetration in transmission networks) and to implement TSO adjustment actions with the aim of managing/monitoring power flow solutions (*e.g.*, controlling tap positions of PST or OLTC transformers).

For the network elements, suitable 2-port admittance models are adopted, like the classical π-circuit representations which refer to the equivalent positive sequence single-circuit.

In this way, the building of $\underline{\boldsymbol{Y}}$ matrix can be easily achieved from input data (also collected in matrix form).

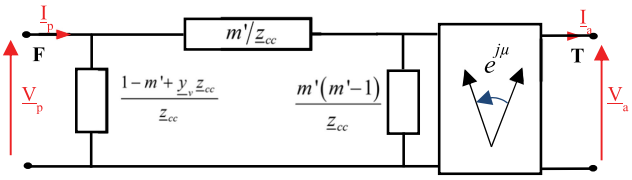

Fig. 11. General p.u. π-model of the two-winding transformer of a given vector group.

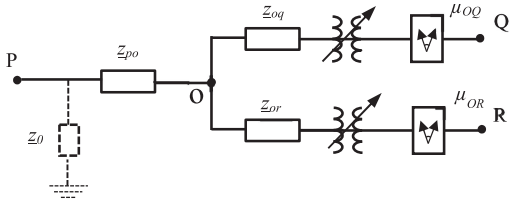

Fig. 12. Representation of three-winding transformer circuit model.

A. Control Power Transformers: OLTC and PST

A generalized two-winding transformer model with shifting complex turn ratio is implemented. Thus, it is possible to characterize both PST and OLTC devices: the former is considered simply as a 1:1 transformer with a given shift angle, whereas the latter is considered as a changeable ratio transformer with a specified tap setting. Starting from the equivalent positive sequence representation, the transmission matrix cascade of each admittance leads to the π-model representation, whose p.u. parameters are presented in Fig. 11. In Fig. 11, three categories of parameters basically appear: firstly, the parameters depending on the specific regulation (generally achieved by using tap changers), which are transformer-voltage ratio and transformer-shift (lag) angle, given respectively by:

$$m' = 1 + \frac{\Delta r\,(tap.position)}{100} \tag{A1}$$

$$\mu_{FT} = \mu_0 \pm \mu\,(tap.position)\,, \tag{A2}$$

where Δr and μ represent the percentual variation from the nominal magnitude ratio and the angle variation from nominal shift angle, respectively.

Secondly, the parameters that can be considered constant with the regulation, *i.e.*,:

$$\begin{aligned} \underline{z}_{cc} &= \text{ p.u. short-circuit impedance;} \\ \underline{y}_{v} &= \text{ p.u. magnetizing admittance;} \end{aligned}$$

although the possibility of making them dependent upon *m'* and μ could be easily implemented (*e.g.*, leakage transformer impedance depending on *m'* and μ).

Thirdly, the parameters depending on the specific power flow solution are:

$$\begin{aligned} \underline{v}_p, \underline{i}_p &= \text{ Starting-terminal phasors,} \\ \underline{v}_q, \underline{i}_q &= \text{ Final-terminal phasors.} \end{aligned}$$

B. Multi-Winding Transformers

Three-winding transformer models are implemented in p.u. by means of a simplified circuital *star* representation (see Fig. 12).

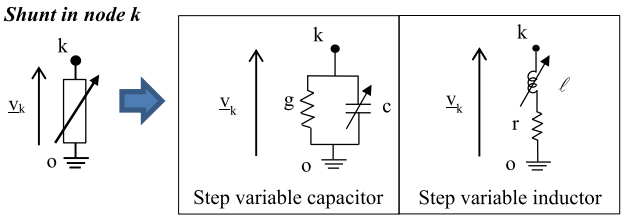

Fig. 13. Representation of the circuit models of shunt devices.

In order to realize the *star* topology, it is necessary to introduce a fictitious centre point *O* connecting *P, Q, R* buses. By considering Fig. 12, the classical parameters modelled are:

$\underline{z}_0$: the magnetizing impedance (generally referred to the higher voltage transformer bus);

$\underline{z}_{PO}$, $\underline{z}_{OQ}$, $\underline{z}_{OR}$: the impedances of star configuration, calculated according to the followings relations

$$\begin{aligned} \underline{z}_{PO} &= \left(\underline{z}_{PQ} + \underline{z}_{PR} - \underline{z}_{RQ}\right)/2 \\ \underline{z}_{OQ} &= \left(\underline{z}_{QP} + \underline{z}_{QR} - \underline{z}_{PR}\right)/2 \\ \underline{z}_{OR} &= \left(\underline{z}_{RP} + \underline{z}_{RQ} - z_{PQ}\right)/2 \end{aligned} \tag{A3}$$

where it is:

$\underline{z}_{PQ} = \underline{z}_{QP}$ = binary short-circuit impedances at the ends of terminal P and Q (on nominal tap positions),

$\underline{z}_{PR} = \underline{z}_{RP}$ = binary short-circuit impedances at the ends of terminal P and R (on nominal tap positions),

$\underline{z}_{QR} = \underline{z}_{RQ}$ = binary short-circuit impedances at the ends of terminal Q and R (on nominal tap positions).

Furthermore, in order to model the changeable voltage complex ratio between transformer terminals, the representation in Fig. 12 may be thought as a combination of three two-winding *star* transformers connected to the common node O. In this way, the three-winding transformer treatment can exploit the above-mentioned theory for two-winding transformers. Thus, binary terminal shift angles (μ_{PQ}, μ_{PR}) depend on the transformers between the terminals OP and OQ:

$$\begin{aligned} \mu_{PQ} &= \mu_{0,OQ} \pm \mu'(tap.position) \\ \mu_{PR} &= \mu_{0,OR} \pm \mu''(tap.position) \end{aligned} \tag{A4}$$

Similarly, binary transformer changeable ratios (m'_{PQ}, m'_{PR}) depend on the transformers between the terminals OP and OQ:

$$\begin{aligned} m'_{PQ} &= 1 + \frac{\Delta r_{OQ}(tap.position)}{100} \\ m'_{PR} &= 1 + \frac{\Delta r_{OR}(tap.position)}{100} \end{aligned} \tag{A5}$$

C. Shunt Devices: Reactive Compensations and Power Factor Correction Capacitances

Shunt compensators and filters are represented as shunt admittances. These devices are fundamental in the real networks, in order to control the reactive power circulation and to adjust voltage profiles. There are many parallel/series modular configurations that can be easily considered; however, the most common layouts for transmission grids are shown in Fig. 13. The tap changer acts so to modify reactive power absorption, by changing the physical values of ℓ and c. The admittances $\underline{y}_{ko}$ are related to shunt devices in *k* node and depend on the specific regulation, so, for the two examples of Fig. 13, it is possible to write:

$$\begin{aligned} \underline{y}_{ko,c} &= f[c(tap.position), g] \\ \underline{y}_{ko,l} &= f[\ell(tap.position), r]. \end{aligned} \tag{A6}$$

Parameters *r* and *g* are instead supposed constant with the voltage.

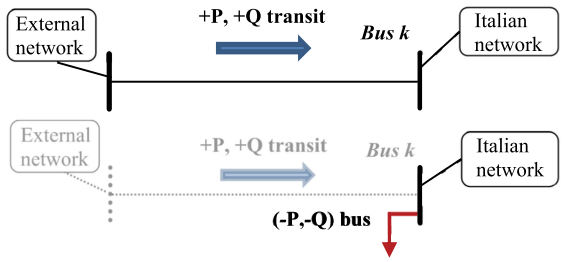

Fig. 14. Modelling of the injection of active/reactive power by means of a PQ constraint.

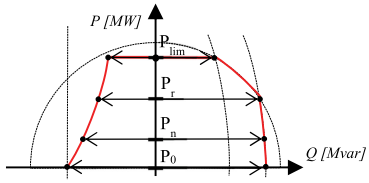

P [MW]	P_0	...	P_{an}	...	P_r	...	P_{lim}
Qmin [Mvar]	$Q_{min,0}$	...	$Q_{min,n}$	...	$Q_{min,r}$	...	$Q_{min,lim}$
Qmax [Mvar]	$Q_{max,0}$	...	$Q_{max,n}$	...	$Q_{max,r}$	...	$Q_{max,lim}$

Fig. 15. Capability curve, built from tabular data, by means of the spline interpolation.

D. Distributed Generations and Interties

Both distributed generation scenarios [33] and interconnections with external grids can be modelled in PFPD. This is performed by considering the involved network nodes *k* as dispatchable PQ buses.

However, since PQ nodes are generally used to model load buses, it is important to schedule power constraints by changing the sign of the active and reactive power.

Fig. 14 shows the treatment of a generic node *k* receiving active/reactive power from an external grid.

Moreover, the ever-growing presence of devices able to inject reactive power can be treated as dispatchable PQ buses (limitedly to the steady-state power flow), *e.g.*: mechanical rotating compensators or static var compensators (SVC).

E. Capability Curves

The capability curve of each generator is stored in PFPD: the algorithm associates a safe operation reactive power range with each generated active power, from a minimum *var* value to a maximum one, as shown in Fig. 15. Capability curves are obtained by means of spline interpolation of tabular (P, Q) data (see Fig. 15). Thus, the adjustments on generator power limits are implemented by considering the stored capability curves. In

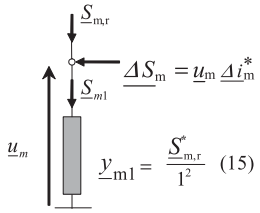

Fig. 16. PQ bus m characterized by its nominal admittance $\underline{y}_{\mathrm{m1}}$ and constrained complex power $\underline{S}_{\mathrm{m,r}}$.

fact, the generators which exceed *var* limit after the first power flow calculation can be forced to generate the associated Q_{lim} by treating them as PQ buses [33].

APPENDIX B

The simplification of the iterative correcting current formulation is one of the most advantageous effects of modelling the slack bus as a shunt admittance. The generalization of (8) and (9) yields:

$$\underline{\boldsymbol{\Delta i}}_{\boldsymbol{G}} = \underline{\boldsymbol{Y}}_{\boldsymbol{GG}}\underline{\boldsymbol{u}}_{\boldsymbol{G}} + \underline{\boldsymbol{Y}}_{\boldsymbol{GL}}\underline{\boldsymbol{u}}_{\boldsymbol{L}} \tag{A7}$$

$$\underline{\boldsymbol{\Delta i}}_{\boldsymbol{L}} = \underline{\boldsymbol{Y}}_{\boldsymbol{LG}}\underline{\boldsymbol{u}}_{\boldsymbol{G}} + \underline{\boldsymbol{Y}}_{\boldsymbol{LL}}\underline{\boldsymbol{u}}_{\boldsymbol{L}}. \tag{A8}$$

Starting from (A7) and (A8), the following matrix partitioning presented in [17] can be avoided:

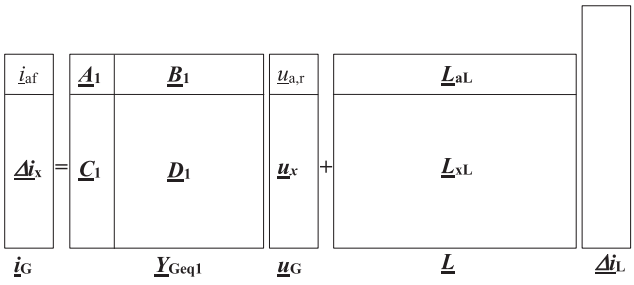

This matrix partitioning in [17] is unnecessary if the slack bus is treated as a quasi-ideal current source. In fact, PFPD allows a unique synthetic formulation valid for all the generators in the network, *i.e.*,:

$$\underline{\Delta i}_{\mathbf{G}} = \left[\underline{\boldsymbol{Y}}_{\mathbf{GG}} - \underline{\boldsymbol{Y}}_{\mathbf{GL}}\underline{\boldsymbol{Y}}_{\mathbf{LL}}^{-1}\underline{\boldsymbol{Y}}_{\mathbf{LG}}\right]\underline{\boldsymbol{u}}_{\boldsymbol{G}} + \underline{\boldsymbol{Y}}_{\mathbf{GL}}\underline{\boldsymbol{Y}}_{\mathbf{LL}}^{-1}\underline{\Delta i}_{\mathbf{L}} \tag{A9}$$

Equations (16), and (17) can be easily obtained by (29), which is the formula (19) with the extended version of $\underline{\boldsymbol{Y}}_{\boldsymbol{Geq}}$.

By observing Fig. 16, in order to obtain (18) the application of the constrained complex power $\underline{S}_{m,r}$ (in PQ nodes) gives

$$\underline{\Delta S}_{m} = \underline{S}_{m1} - \underline{S}_{m,r} \tag{A10}$$

which can be written as a function of the computed voltage in (17):

$$\underline{u}_{m}\underline{\Delta i}_{m}{}^{*} = |\underline{u}_{m}|^{2}\cdot\underline{y}_{m1}^{*} - 1^{2}\cdot\underline{y}_{m1}^{*} \tag{A11}$$

hence the correcting current at m PQ node is given by:

$$\underline{\Delta i}_{m} = \underline{y}_{m1}\cdot\frac{|\underline{u}_{m}|^{2} - 1}{\underline{u}_{m}^{*}} \tag{A12}$$

By generalizing (32) for all the PQ admittances, the following vectorial expression can be written

$$\underline{\boldsymbol{\Delta i}}_{\mathbf{L}} = \left(diag\left(\underline{\boldsymbol{Y}}_{\mathbf{L}}\right)/\underline{\boldsymbol{u}}_{\mathbf{L,c}}^{*}\right)\otimes\left(\left|\underline{\boldsymbol{u}}_{\mathbf{L,c}}\right|^{2} - \mathbf{1}\right) \tag{A13}$$

where $\mathbf{1}$ is the array of ones and diag($\underline{\boldsymbol{Y}}_{\mathbf{L}}$) is the main diagonal vector of $\underline{\boldsymbol{Y}}_{\mathbf{L}}$. In order to obtain (20), (29) gives the correcting current vector of all the generators (including the slack one). However, its quadrature components must be obtained only for PV buses. The imaginary part of the complex power vector is given by:

$$\mathrm{j}\boldsymbol{\Delta q}_{\mathbf{G}} = \mathrm{j}\ \left[Im\left(\underline{\boldsymbol{u}}_{\mathbf{G}}\otimes\underline{\boldsymbol{\Delta i}}_{\mathbf{G}}^{*}\right)\right]. \tag{A14}$$

By considering the quadrature component correcting current vector $\underline{\boldsymbol{\Delta i}}_{\mathrm{G,c\_q}}$ springing out of the same injection of reactive power, it must also satisfy the following

$$\underline{\boldsymbol{u}}_{\mathrm{G,c\_q}}\otimes\underline{\boldsymbol{\Delta i}}_{\mathrm{G,c\_q}}^{*} = j\left[\ Im\left(\underline{\boldsymbol{u}}_{\boldsymbol{G,c\_q}}\otimes\underline{\boldsymbol{\Delta i}}_{\boldsymbol{G,c\_q}}^{*}\right)\right]. \tag{A15}$$

From (35), it is immediate to obtain (36) which is (20):

$$\underline{\boldsymbol{\Delta i}}_{\mathrm{G,c\_q}} = -j\left[Im\left(\underline{\boldsymbol{u}}_{\mathrm{G,c\_q}}\otimes\underline{\Delta i}_{\mathrm{G,c\_q}}^{*}\right)\right]/\underline{\boldsymbol{u}}_{\boldsymbol{G,c\_q}}^{*}. \tag{A16}$$

vv

ACKNOWLEDGMENT

The author gratefully acknowledges Dr. G. M. Giannuzzi, Dr. R. Zaottini and Dr. N. Crocamo for sharing the Digsilent Projects of Italian grid. Moreover, the author warmly acknowledges Dr. Giovanni Gardan, Dr. Sebastian Dambone Sessa, Dr. Francesco Sanniti, Dr. Luca Rusalen, Dr. Simone Talomo and Dr. Nicola Renesto for their fruitful discussions about the paper.

REFERENCES

[1] H. E. Brown, G. K. Carter, H. H. Happ, and C. E. Person, "Power flow solution by impedance matrix iterative method," *IEEE Trans. Power Appl. Syst.*, vol. 82, no. 65, pp. 1–10, Apr. 1963.

[2] H. W. Hale and R. W. Goodrich, "Digital computation of power flow - Some New aspects," *AIEE Trans. Power App. Syst.*, vol. 78, no. 3, pp. 919–923, Apr. 1959.

[3] W. F. Tinney and C. E. Hart, "Power flow solution by newton's method," *IEEE Trans. Power Appl. Syst.*, vol. 86, no. 11, pp. 1449–1460, Nov. 1967.

[4] B. Stott and O. Alsaç, "Fast decoupled load flow," in *Proc. IEEE PES Summer Meeting*, 1973, Art. no. T 73 463-7.

[5] B. Stott, "Review of load-flow calculation methods," *Proc. IEEE*, vol. 62, no. 7, pp. 916–929, Jul. 1974.

[6] J. Arrillaga and C. P. Arnold, *Computer Analysis of Power Systems*. England: John Wiley and Sons, 1990.

[7] M. Carpentier, "Application de la méthode de newton au calcul des résaux maillés," in *Proc. Power Syst. Comput. Conf.*, London, 1963, pp. 365–375.

[8] S. Iwamoto and Y. Tamura, "A load flow calculation method for ill-conditioned power systems," *IEEE Trans. Power Appl. Syst.*, vol. PAS-100, no. 4, pp. 1736–1743, Apr. 1981.

[9] F. Milano, "Continuous newton's method for power flow analysis," *IEEE Trans. Power Syst.*, vol. 24, no. 1, pp. 50–57, Feb. 2009.

[10] B. Liu, J. Li, H. Ma, and Y. Liu, "Generalized benders decomposition based dynamic optimal power flow considering discrete and continuous decision variables," *IEEE Access*, vol. 8, pp. 194260–194268, 2020.

[11] J. Lavaei and S. H. Low, "Zero duality gap in optimal power flow problem," *IEEE Trans. Power Syst.*, vol. 27, no. 1, pp. 92–107, Feb. 2012.

[12] M. Geidl and G. Andersson, "Optimal power flow of multiple energy carriers," *IEEE Trans. Power Syst.*, vol. 22, no. 1, pp. 145–155, Feb. 2007.

[13] J. A. Momoh, R. Adapa, and M. E. El-Hawary, "A review of selected optimal power flow literature to 1993. I. Nonlinear and quadratic programming approaches," *IEEE Trans. Power Syst.*, vol. 14, no. 1, pp. 96–104, Feb. 1999.

[14] J. Arrillaga, "DC versus AC transmssion," in *High Voltage Direct Current Transmission*, 1st ed, UK: IEE Power Engineering Series 6, Peter Peregrinus Ltd., 1983.
[15] J. Arrillaga and P. Bodger, "AC-DC load-flow with realistic representation of the converter plant," *Proc. IEE*, vol. 125, no. 1, pp. 41–46, Jan. 1978.
[16] A. Tosatto, T. Weckesser, and S. Chatzivasileiadis, "Market integration of HVDC lines: Internalizing HVDC losses in market clearing," *IEEE Trans. Power Syst.*, vol. 35, no. 1, pp. 451–461, Jan. 2020.
[17] R. Benato, A. Paolucci, and R. Turri, "Power flow solution by a complex admittance matrix–Method," *Eur. Trans. Elect. Power*, vol. 11, no. 3, pp. 181–188, 2001.
[18] M. Baradar and M. R. Hesamzadeh, "AC power flow representation in conic format," *IEEE Trans. Power Syst.*, vol. 30, no. 1, pp. 546–547, Jan. 2015.
[19] M. Vanin, H. Ergun, R. D'hulst, and D. Van Hertem, "Comparison of linear and conic power flow formulations for unbalanced low voltage network optimization," *Electr. Power Syst. Res.*, vol. 189, no. 5, pp. 1–8, 2020.
[20] S. D. Manshadi, G. Liu, M. E. Khodayar, J. Wang, and R. Dai, "A convex relaxation approach for power flow problem," *J. Mod. Power Syst. Clean Energy*, vol. 7, no. 6, pp. 1399–1410, 2019.
[21] D. K. Molzahn and I. A. Hiskens, "A survey of relaxations and approximations of the power flow equations," *Foundations Trends Electr. Energy Syst.*, vol. 4, pp. 1–221, 2019.
[22] C. Coffrin, H. L. Hijazi, and P. Van Hentenryck, "The QC relaxation: A theoretical and computational study on optimal power flow," *IEEE Trans. Power Syst.*, vol. 31, no. 4, pp. 3008–3018, Jul. 2016.
[23] M. S. Andersen, A. Hansson, and L. Vandenberghe, "Reduced-complexity semidefinite relaxations of optimal power flow problems," *IEEE Trans. Power Syst.,* vol. 29, no. 4, pp. 1855–1863, Jul. 2014.
[24] B. park, M. C. Ferris, and C. L. DeMarco, "Benefits of sparse tableau over nodal admittance formulation for power-flow studies," *IEEE Trans. Power Syst.*, vol. 34, no. 6, pp. 5023–5032, Nov. 2019.
[25] M. Usman, A. Cervi, M. Coppo, F. Bignucolo, and R. Turri, "Cheap conic OPF models for low-voltage active distribution networks," *IEEE Access*, vol. 8, pp. 99691–99708, 2020.
[26] R. García-Blanco, D. Borzacchiello, F. Chinesta, and P. Diez, "Monitoring a PGD solver for parametric power flow problems with goal-oriented error assessment," *Int. J. Numer. Methods Eng.*, vol. 111, no. 6, pp. 529–552, 2017.
[27] D. Borzacchiello, F. Chinesta, M. H. Malik, R. García-Blanco, and P. Diez, "Unified formulation of a family of iterative solvers for power systems analysis," *Electr. Power Syst. Res.,* vol. 140, pp. 201–208, 2016.
[28] K. Sunderland, M. Coppo, M. Conlon, and R. Turri, "A correction current injection method for power flow analysis of unbalanced multiple-grounded 4-wire distribution networks," *Electr. Power Syst. Res.,* vol. 132, pp. 30–38, 2016.
[29] V. C. Strezoski and P. M. Vidovic, "Power flow for general mixed distribution networks," *Int. Trans. Elect. Energy Syst.,* vol. 25, no. 10, pp. 2455–2471, 2015.
[30] A. Vinkovic and R. Mihalic, "A current-based model of an IPFC for newton-raphson power flow," *Electr. Power Syst. Res.,* vol. 79, no. 8, pp. 1247–1254, 2009.
[31] F. M. Gatta, A. Geri, S. Lauria, and M. Maccioni, "Improving high-voltage transmission system adequacy under contingency by genetic algorithms," *Electr. Power Syst. Res.*, vol. 79, no. 1, pp. 201–209, 2009.
[32] DIgSILENT PowerFactory, 2021. [Online]. Available: http://digsilent.de/
[33] R. Zimmerman, C. Murillo-Sanchez, and R. Thomas, "MATPOWER: Steady-state operations, planning and analysis tools for power systems research and education," *IEEE Trans. Power Syst.,* vol. 26, no. 1, pp. 12–19, Feb. 2011.
[34] G. Granelli and M. Montagna, "MATLAB implementation of the complex power flow," *COMPEL*, vol. 32,no. 3, pp. 923–935, 2013.
[35] F. L. Alvarado, "Solving power flow problems with a matlab implementation of the power system applications data dictionary," in *Proc. 32nd Annu. Hawaii Int. Conf. Syst. Sci.*, Maui, HI, USA, 1999, Art. no. 7.
[36] I. Abduleahman, "Matlab-Based programs for power system dynamic analysis," *IEEE Open Access J. Power Energy*, vol. 7, pp. 59–69, 2019.
[37] J. Mahseredjian and F. Alvarado, "Creating an electromagnetic transient program in matlab: MatEMTP," *IEEE Trans. Power Del.*, vol. 12, no. 1, pp. 380–388, Jan. 1997.
[38] F. Milano, "An open source power system analysis toolbox," *IEEE Trans. Power Syst.*, vol. 20, no. 3, pp. 1199–1206, Aug. 2005.
[39] J. Stewart, "Limits and Derivatives," in *CALCULUS Early Transcendentals,* 8th ed., Boston, USA: CENGAGE Learning, 2014.
[40] F. Milano, *Power System Modeling and Scripting*, London, UK: Springer-Verlag, Power Systems Series, 2010.
[41] T. J Overbye, "A power flow measure for unsolvable cases," *IEEE Trans. Power Syst.*, vol. 9, no. 3, pp. 1359–1365, Aug. 1994.
[42] M. M. M. El-Arini, "Decoupled power flow solution for well-conditioned and ill-conditioned power systems," *IEE Proc.-C*, vol. 140, no. 1, pp. 7–10, Jan. 1992.
[43] R. Benato *et al.*, "An original educational algorithm assessing the behaviours of angular frequency deviations of a multimachine system in small signal analysis," *IEEE Access*, vol. 9, pp. 18783–18800, 2021.
[44] R. Benato and A. Paolucci, *EHV AC Undergrounding Electrical Power: Performance and Planning*, London, UK: Springer-Verlag London Limited, 2010, pp. 29–32.

Roberto Benato (Senior Member, IEEE) was born in Venezia, Italy, in 1970. He received the Dr. Ing. degree in electrical engineering from the University of Padova, Padua, Italy, in 1995 and the Ph.D. in power systems analysis in 1999. In 2011, he was appointed as an Associate Professor with the Department of Industrial Engineering, Padova University. He is the author of 200 papers and four books, edited by Springer, Wolters Kluwer, and China Machine Press. He is a Member of six Cigré Working Groups (WGs) and secretary of two Joint WGs, and Member of IEEE PES Substations Committee. In 2014, he was nominated Member of IEC TC 120 Electrical Energy Storage (EES) Systems in the WG 4 Environmental issues of EES systems. He is currently a corresponding Member of Cigré WG B1.72 Cable rating verification 2nd part. In 2018, he is elevated to the grade of CIGRÉ Distinguished Member. He is a Member of Italian AEIT.